Mechanical testing and osteointegration of titanium implant with calcium phosphate bone cement and autograft alternatives

Lin, Dan-Jae, Department of Dental Hygiene, China Medical University, Taichung, Taiwan 40402, R.O.C

Ju, Chien-Ping, Department of Materials Science and Engineering, National Cheng-Kung University, Tainan, 701, Taiwan, ROC

Huang, Shu-Huei, Department of Materials Science and Engineering, National Cheng-Kung University, Tainan, 701, Taiwan, ROC

Tien, Yin-Chun, Department of Orthopaedics, Kaohsiung Medical University Hospital, Kaohsiung, 807, Taiwan, ROC

Yin, Hsiang-Shu, Department of Anatomy and Cell Biology, College of Medicine, National Taiwan University, Taipei, 100, Taiwan, ROC

Chen, Wen-Cheng*, Department of Fiber and Composite Materials, Feng Chia University. Taichung, 40724, Taiwan, ROC

Chern Lin, Jiin-Huey*,Department of Materials Science and Engineering, National Cheng-Kung University, Tainan, 701, Taiwan, ROC

Correspondence:
Chen, Wen-Cheng
Department of Fiber and Composite Materials, Feng Chia University.
100, Wenhwa Rd., Seatwen,
Taichung,40724, Taiwan (ROC)
Tel/fax: +886-4-24517250 ext 3413/
+886-4-24514625
e-mail: wincheng0925@yahoo.com.tw

Chern Lin, Jiin-Huey
Department of Materials Science and Engineering, National Cheng-Kung University, Tainan, 701, Taiwan, ROC
Tel/Fax: 886-6-274-8086
e-mail: chernlin9@gmail.com

Mechanical testing and osteointegration of titanium implant with calcium phosphate bone cement and autograft alternatives

Abstract

The purpose of this study was to evaluate the osteointegration of a titanium (Ti) implant with the calcium phosphate cement (CPC) and autograft prostheses by pull-out test and histological examination. Stems of sixty Ti cylinders were bilaterally inserted into femoral medullary canals in 30 rabbits at the 1st, 4th, 12th, 26th and 70th postoperative week. The bone autograft and CPC were filled into the pre-trimmed bone marrow cavity with a polymethyl-methacrylate retarder in the distal end, and then a Ti cylinder was inserted into femurs. The CPC group was significantly ($p<0.05$) associated with a larger pull-out force at 4th (37%) and 12th (62%) week compared to the autograft group. The bone area and the bone-to-implant contact ratios of the CPC groups were significantly higher than that of the autograft groups at early healing stage. The histological exams suggest that the CPC enhanced the earlier bone formation around the implant at the period not longer than 12 weeks post-operation. We conclude that CPC graft has the higher ability to facilitate the osteointegration and stabilize the Ti implant at a relatively early stage than the autograft *in vivo*.

Keywords: Autograft; Calcium phosphate bone cement; Titanium implant; Pull-out test; Osteointegration

Introduction

Bone or bone-like materials used in bone grafts may come from patent-self (bone autograft), from a donor (allograft) or from a man-made and synthetic source such as the demineralized bone matrix, ceramics, polymethyl methacrylate (PMMA), calcium phosphate bone cements (CPC) and so on.

Osteointegration is an important point of assessment for the success of hard tissue replacement prostheses and fixation implant surgeries. The interface bonding forces that determine the success of osteointegration derive from two elements, namely, the mechanical interlocking and the biological bonding of growing bone tissue to the implant. Implants with roughened or porous surface coatings are known to provide superior mechanical interlocking with the surrounding bone and achieve higher stability. On the other hand, biological bonding, which strongly affects an implant's long-term stability, is more closely related to the implant material itself. Titanium (Ti) and its alloys can be extremely inert to corrosion and are widely used as implant stems [1]. Coatings with calcium phosphates may be enhancing bone ingrowth early in the ingrowth phase [2, 3], but the coatings are liable to peel off from the substrate; as a result the delaminated hard debris would eventually lead to chronic inflammation and implant failure [4-6].

The success of osteointegration in the clinical setting not only depends on the surface characteristics of the implant but is also strongly affected by the patient's bone condition and the geometric fit [7]. In most cases, the bone autografts that are transplanted directly from one area of an individual's skeleton or residual bone tissues are the preferred way to use. However, patients with poor bone quality may fail to achieve initial stability or lead to another fracturing problem in comparison to normal patients, and the former group tends to exhibit delayed osteointegration and a higher

failure rate [8-11]. Anatomic variation causes inadequate fitness (i.e., geometric mismatches between the prosthesis and the bone matrix) and may cause severe instability as a result of the micromovement that occurs when the prosthesis bears load [12-14].

PMMA is a general cementing material for grouting to the prosthesis in clinical applications [15]. However, the exothermic reaction during PMMA polymerization and the thereafter shrinkage may be harmful to osteointegration [16] . Moreover, the biocompatibility benefit of a Ti implant is also negatively impacted by the presence of PMMA cement. Several studies have attempted to improve the biocompatibility and long-term stability of cemented fixations by using incorporated some additives into acrylic bone cement for diverse purposes. Examples include oligomer fillers based on amino acid (Puska et al., 2003), radiopaque agents (van Hooy-Corstjens et al., 2007), bioactive $CaO\text{-}SiO_2$ based glasses (Boesel et al., 2007), antibiotics (Frutos et al., 2010), carbon nanotubes (Ormsby et al., 2010), and titania nanotube (Khaled et al., 2010) that have been discovered as an additive in acrylic bone cement.

Due to its superior biocompatibility and osteoconductivity, CPC has been proposed as a filling material in dental and orthopedic applications [17-19]. CPC with a final product of hydroxyapatite (HA) is commonly a mixture of two pre-mixed Ca/P powders (tetra-calcium phosphate (TTCP)/dicalcium phosphate anhydrous (DCPA) or dihydrate (DCPD)) and a diluted phosphate-containing solution [20, 21]. Apatite is the main inorganic content of natural human bone and CPC after implantation will be resorbed partially [22, 23]. The injectable and in-situ hardening features plus excellent bone affinity make CPC a good candidate for bone regeneration in many clinical applications. In vitro studies have demonstrated that the initial stability of various types of prosthetic fixations can be increased with CPC injection [24, 25]. However,

the mechanical evaluation from an osteointegration perspective of an implant with CPC injection in vivo has not been comprehensively studied to date.

Our hypothesis is that geometric mismatches between implant and bone tissues have higher possibility to be overcome by inserting CPC paste into the interfaces than bone autografts and thus enhance the initial stability (reduce micromovement). Furthermore, the CPC should attract osteoprogenitor cells towards the implant and the new regenerated bone will replace the grafted CPC to ensure biological stability.

Materials and methods

We use a non-dispersive bone cement (nd-CPC) which was demonstrated to have a non-dispersive feature by treating the reactant particles of TTCP/DCPA-based cement with nanocrystallites on the surfaces [26]. The detailed procedures has been described in our previous studies (Wang et al., 2010) and a US patent No. 7094282. Briefly, after the preparation CPC of well mixing equimolar in-house fabricated TTCP (mean particle size 12.6 μm) and mechanical grinded DCPA (2.1μm) powders, the nd-CPC was fabricated from powders containing 5 g of CPC, which are stirred in 1.6 mL of 0.25 mM phosphoric acid for 1 min. The resulting mixture was then dried and mechanically ground. The final mean particle size of original nd-CPC powder was 6.6 μm. The nd-CPC powders and hardening solution (25 mM phosphate, pH was 1.96) were sterilized by incubation for 30 min at 160 ^{o}C and autoclaving for 20 min at 120 ^{o}C, respectively. The powder/hardening liquid ratio of CPC for implantation was 4.0 g/mL. The Ti alloy rods were melted, cast and machined to 3 mm diameter and 40 mm length cylinders. In order to ensure that the measured maximum pull-out forces are associated with the biological bonding of bone tissue and implant, the implants were published and acid etched to guarantee a uniform, smooth surface. The fabrication method for these Ti alloy implants has been described in our previous

paper [27].

Our animal study was performed at Kaohsiung Medical University Animal Center, Kaohsiung, Taiwan. Thirty New Zealand white rabbits (2.5~3.5 kg) were tested. Injection sites were shaved and cleansed with 70% ethanol and Betadine^{TM} (povidone iodine 10%). All animals were operated on under general anesthesia, and experiments were conducted in accordance with the guidelines of the animal research committee of Kaohsiung Medical University. We drilled a 3.5 mm diameter and 35 mm length cylindrical guiding hole from the distal end of the femur and collected the residuals of bone marrow and debris of bone tissues from the drilled femur surface and driller. We then placed a 5 mm PMMA block at the bottom of the guiding hole as a retarder to prevent the bone grafts from leaking out (relative positions are shown in Figure 1). The CPC paste was prepared by mixing the nd-CPC powders with the hardening solution for 1 min. The collected autograft and the CPC paste were then loaded into the 3 mL-syringes individually. The injection of CPC (right leg) and autograft (left leg) were performed by moving the syringes carefully from the bottom to the surface of the defect. Once the bone grafts had been filled into the holes, we inserted the Ti stem in and wiped the excess grafts away from the joint plane. Four rabbits were sacrificed for the pull-out tests and two for histological samples at the 1st, 4th, 12th, 26th and 70th postoperative week. The bilateral femurs were retrieved, and the soft tissue was cleaned gently. The samples were then kept in 4 ^{o}C PBS and were subjected to mechanical and histological testing randomly.

For mechanical testing, the condyle was excised to expose the internal screw, and all samples were tested within 8 hours after scarification. The pull-out test was carried out (n=4) using a tester (Shimadzu AGS-500D, Kyoto, Japan) operating at a crosshead speed of 0.5 mm/sec. The peak load was recorded automatically until the

implant had been fully extracted (Fig. 2). The maximum forces (kgf) of different implanted time were analyzed using one-way ANOVA followed by Tukey's post-hoc comparison.

For histology, the retrieved samples were sectioned followed with formalin fixation immediately for both decalcified paraffin and non-decalcified plastic embedding. The detail are described below, the femurs were sectioned perpendicular to the long axis (5 mm thick) using a Buehler low-speed diamond saw at sections I, II, III (two slices per site) as shown in Fig. 1. For the decalcified samples, the sectioned bone tissue was fixed, decalcified and then the Ti stem was removed gently with tweezers, followed by a series of alcoholic dehydrations. After embedding in paraffin, 5 μm-thick sections of the sample were obtained using a rotary microtome. The slices were then plated, deparaffinized and stained with routine hematoxylin and eosin (H&E). Immunohistochemical (IHC) staining was carried out as detailed in a previous protocol [27]. Briefly, the paraffin sections were deparaffinized and blocked with 1.25% normal serum before incubation with anti-vitamin D receptor or anti-vimentin antibodies (Sigma, St. Louis, USA), diluted 1:500 or 1:100 in PBS, for 16 h at 4 ^{o}C. The anti-vitamin D receptor antibody labels the osteoblasts/osteoclasts (the vitamin D receptor is present on the membrane of osteo-related cells), and the anti-vimentin antibody labels the cell skeleton. Thereafter, the samples were incubated with a biotinylated secondary antibody, followed by visualization of immunoreaction products by the ABC-peroxidase method (Vector) using 3,3'-diaminobenzidine tetrahydrochloride (DAB) as the chromagen. We used the Image Pro software package to determine the total bone area (BA, in %) and the bone-to-implant contact ratios (BIC, in %) from combined pictures of the 10X objective lens [28]. The BA was defined as the percentage of bone contact areas around the implant (within a

predefined 4 mm diameter circle) (n=4).

For the non-decalcified samples, the sectioned bone was fixed, dehydrated, embedded in MMA, and sectioned to a thickness of 250 μm. Sections were thinned out to a final thickness of 60 μm, polished and glued to slides with Permount (Fisher Scientific, Fair Lawn, NJ, USA). The sections were then stained with toluidine blue for optical microscopy or with Villanueva Bone Stain (Polysciences Inc., Pennsylvania USA) for laser confocal microscope (Leica TCS SP2, Wetzlar, Germany) observation.

Results

Maximum pull-out forces

The pull-out forces of the CPC groups were gradually increased over time and the average values at the 4, 12 and 70th week were 7.0, 24.1 and 41.2 kgf, respectively (Fig. 3). Statistical analyses showed that these forces differed significantly in both CPC and autograft groups at different implantation times ($p<0.0001$). The pull-out forces of the CPC group were significantly greater than autograft group at the 4th week by 37% ($p<0.05$) and at the 12th week by 62% ($p<0.001$) but the forces are no significance between the two groups at long-term implantation ($p>0.05$ for 26th and 70th postoperative weeks).

Histological results

The femurs were X-rayed before sectioning and by assessing the X-ray images of the 1st week implantation (Fig. 4), we concluded that there were tissues attached to the implants of both groups in the distal side. However, from the cross-section view, some tissues seemingly left a large space aside the implant in the autograft group (Fig. 4a sections I and II). The inner side of the tissues exhibited the same curvature as the

implant (arrowhead in sections I and II) implying that movement may have occurred after implantation of the Ti implant with autografts. The radio-opaque areas (arrows in Fig. 4b) close to the peripheral implant provide evidence of the presence of residual CPC paste.

Figure 5 shows H&E stained specimen of the CPC and autograft groups for sections II and PMMA parts for sections III. For section II in the autograft group, there was apparent fibrous stroma around the Ti stem (Fig. 5a) till to 12th week implantation. By 4th week, woven new bone and small capillaries were apparent near the implant (Fig. 5b). After 12th week, the new bones became more compact and had larger areas than at 4th week (Fig. 5c).

By contrast, when the Ti implant was inserted with CPC paste, the isolated island of CPC pastes were immediately captured by the new bone in the medullary region around the implant (Figs. 5d-f) just at 1st week implantation. The CPC conducted and merged into the peripheral new bone over time. The thicker and compact bone tissues around the implant of the CPC and autograft groups were observed after 12 weeks. There still exist visible fibrous tissues between the implant and new bone in the autografts but is not seen in the CPC groups at any time points. The bone marrow around the PMMA was accompanied by necrosis and hematoma at 1st postoperative week. After 4 and 12 weeks, a few fibrous tissues were existed beside the PMMA and still exhibited chronic inflammation (Figs. 5g-i).

Figure 6 shows the new bone areas (BA, in %) around the implants and bone-to-implant contact ratios (BIC, in %) of both the CPC and autograft groups. The mean BA % of both groups increased over time. By comparison of the two groups, we found the BA % of the CPC were significant larger than autograft groups at 1st, 4th, and 12th week ($p<0.05$). However, statistically analysis of the BA % between the two

groups are similar after a long-term implantation; $p>0.05$ for BA % between 12th, 26th, 70th week of CPC groups and between 26th and 70th week of autograft groups.

Same tendencies as BA % are shown in the results of BIC ratios. The BIC % of the CPC groups through the time are significantly different ($p<0.001$). There are also significantly differences between the BIC % of the autografts ($p<0.001$) over time. By Tukey's comparison, the CPC groups have a significantly higher BIC % than the autografts at 1st, 4th, and 12th weeks ($p<0.05$). Noteworthy, the BIC % of the CPC group was reached the plateau at an early implantation time of 4th week but the autograft group was delayed till the 26th week. The BIC % of the CPC group at 4th week (80.4%) is significantly higher than that of autograft at 12th postoperative week (64.3%).

The non-decalcified stained sections clearly revealed the interface between the growing tissues and the CPC/implant (Fig. 7). Abundant cement around the Ti was bordered by new bone and some loose or isolated cement particles were observed. These cement particles were captured by multi-nuclear macrophages (arrow in Fig. 7b). The CPC was replaced by new bone near the periphery of the Ti at 12th postoperative week (Fig. 7c). The residual cement "island" near the implant was completely covered by peripheral trabecular bone, and the edge of the remaining cement seemed more round than it had been at 1st postoperative week. The CPC seems to have been replaced by the new gradually forming bone (Figure 7d), and the edge of the cement was fused by a new osteon formation (asterisk).

Osteoclasts (OC) near the CPC were identified by IHC stain images (Fig. 8). The stained steoclasts (OC) coexist with osteoblasts (Ob) (arrowhead) at the cement/bone interface, demonstrating that the bone exhibited higher activity. The normal bone remodeling was occurring. The subsurface of fluorescence-stained

(Villanueva Bone stain) sections generate in Fig. 8c. That shows a progenitor cell (Pc) from bone marrow into a cement crevice at 4th postoperative weeks. After 12 weeks, the structures of attached bones became mature and laminar (Fig. 8d), and the osteocytes (Os) in the lacuna were very close to the cement. The border of the laminar bone (mineralized bone is a blackish-green color) was intermixed with a layer of osteoid/collagens that was stained a fluorescent pink color under the excitation laser (488/543 nm). On the other side, the CPC appeared in loose clusters (light blue stained), and the porosity of the remaining cement was degraded towards the bulk of the cement area.

Discussion

We found that when the prosthesis was implanted together with a CPC, the pull-out forces were significantly greater at the early bone regenerated stages of 4th and 12th week implantation in the CPC than in the autografts. The increased pull-out forces are attributed to the higher BIC and BA ratios. That means more forces are needed to peel-off the osteointegrated bone tissues from the Ti implant. The histological fresh sections in autografts (Fig. 4a) showed a gap between the Ti implant and the ongrowth tissues at 1st week, suggesting that major movement may have occurred to induce the tissue to detach from the implant at early regeneration. Micromotion between bone and implant can inhibit bone ingrowth and results in a fibrous membrane [12, 29, 30]. The phenomena of fibrous captures were also observed in the 1st and 4th week histological results of the autograft groups.

On the contrary, when the CPC paste was filled into the cavity between Ti and the cortical bone, the in-situ hardened features of CPC is expected to enhance the stability of the implant and inhibit the micromotions. Our radiographs (Fig. 4b)

revealed that the CPC paste did not form a uniform coating on the Ti prosthesis; instead, it naturally filled up the voids and spaces around the Ti in the environment of bone marrow presence. Because the osteoconductive CPC generate the bone tissue on the Ti surfaces, the CPC graft provided a more stable fixation than for the autograft. The same result of the initial stability of press-fit femoral stems in dog bones would be enhanced by CPC injection [31, 32]. In order to simulate clinical usage, most studies to date have used threaded screws or porous surface prostheses to perform the mechanical testing. Therefore, increased pull-out force readings may be attributed to increasing friction between the cement and the prosthesis and to the force which is need to break the hardened cement itself.

Hoshikara et al. [33] measured the pull-out strength of Ti cancellous screws with and without CPC augmentation and reported that the pull-out forces with CPC injection were greater than those without CPC injection on the following day and at 3rd and 6th week implantation. However, there was no significant difference in the forces at these three implantation time points with CPC. In our study, the pull-out force on the 24 h implantation was even greater in the CPC group than in the without CPC group and made no difference with 6th weeks implantation. This is due to a different implant design and varied implant site. Moreover, their Ti screws were placed into an over-sized drilled hole; the pull-out force they measured represent the breaking strength of CPC/bone or CPC itself but not the strength of implant/bone especially in the early stage.

Our study was using an implant with smooth surfaces to eliminate geometric effects from different screws and focus on the comparision of osseointegrated abilities of CPC and autograft with Ti implant. Therefore, the pull-out data directly reflect the de-bonding forces between the growing bone/implant. The results suggest that the

CPC could stabilize the implant much more firmly than with the autografts. This increased stability can be attributed to the increasing contacting surface (more friction force) of the surrounding bone/CPC composite bed, which facilitates bone ongrowth.

The pull-out strengths and bone contact areas of the two groups increased gradually over time after the operation. We saw significant differences between the pull-out forces of the two groups at 4th and 12th week. Our BA and BIC data also confirm that the significances between CPC and autograft groups are shown at an early stage for 12 weeks implantation. Histological observations show that there is more bone tissue contact around the Ti of CPC group than in the autograft group (Figs. 5, 6) at 1st week. But the increments of BA and BIC % by CPC injection (significantly different between the two groups) are failed to contribute to the pull-out force. We conjectured that although the earlier and larger amount of osteoid formation around the Ti in the CPC than autograft groups, the new osteoid was soft and did not supplement or augment the friction force. Such that the bone tissues contacted on the Ti became gradually mature and rigid over this period. During the stage of 4 to 12 weeks post implantation in the CPC group, more new blood vessels, which serve to supply nutrition to the new bone, together with osteoblast-like cells, were observed in these cement zones and made more contact area of osteoid and Ti. Based on the higher pull-out strength, we conclude that osteointegration occurred earlier in the CPC than in the autograft groups and the effects were special obviously at an early regeneration stage (not longer than 12 weeks post-operation).

Matching of the CPC degradation rates to the bone remodeling rates can be significantly affected the implantation techniques [33, 34]. Our results in this study suggest that with CPC graft for Ti stabilization, more new osteoid had formed at the periphery of the Ti after 1 week. However, a slight inflammatory response, consisting

of a small number of lymphocytes, plasma cells and macrophages, occurred adjacent to fibrous tissue after 1 week implantation in the autograft group.

As studied by Okumura et al. [35], they concluded that bone bonding to HA is associated with undifferentiated stromal stem cell adhesion to the HA surface, followed by osteoblastic differentiation. The consequent surface-dependent cell differentiation results in active osteoblasts that fabricate osteoid directly onto the particle surface. Continual mineralization by the active osteoblasts results in mature bone bonding to the particles and bonding osteogenesis. As shown in our histological images, although some CPC was isolated into the bone spaces, these small particles seemed to be resorbed by the macrophages via the phagocytosis process (Fig. 7b). When the CPC was gradually dissolved or digested by physiological mechanism over time, crevices occurred. That implied CPC cement could act as a scaffold and causes the marrow stromal cells to attach and differentiate into osteoprogenitor cells at 4th week (Fig. 8c). At 4th week, the CPC provide more mechanical stability to the Ti implant as compared to the autografts that was due to the higher significant values of BA and BIC %. And by 12 weeks, a stable and mature contact interface may be generated (Fig. 8d), and this made the largest strength difference with CPC to the autograft group. In addition, bone remodeling begins as osteoblasts aggregate after the CPC has been dissolved by acid phosphate that is released from the osteoclasts, as identified with the IHC stain. The residual CPC was still existed even after 26th postoperative week.

In kyphoplasty, vertebroplasty, orthopedics for the fixation of artificial joints to the host bone, PMMA currently represents the standard in augmentation materials. It is characterized, however, by lack of ossointegration, lower strength and limited biocompatibility. Several efforts (Puska et al., 2003; Boesel et al., 2007; Frutos et al.,

2010; Ormsby et al., 2010; Khaled et al., 2010) have been made to improve the mechanical properties and biocompatibility by the addition of fibers to the cements and mineral particles (e.g. HA, inorganic bone, bioglass, collagen or tricalcium phosphate) to the bone cement to enhance its mechanical strength and biocompatibility respectively. The porous structure on the surfaces of the biomaterials is also needed for new bone ingrowth. The porogen and leaching technique is one of the known methods of fabrication porous scaffolds into polymeric materials (Rezwan et al., 2006). For an example, the addition of resorbable biooligomer to the acrylic bone cement matrix causes porosity formation in a moist environment due to the sorption of water (Puska et al., 2003).

The durability of a cemented anthroplasty is closely related to the quality of fixation of bone cement to the bone, and is also dependent on the interfacial bone between cement and prosthesis (de Waal Malefijt et al., 1987). The bonding between bone and bone cement by interdigitation is the primary mechanical anchorage and the biological reactions in the surrounding tissues following an orthopedic surgeon refer to the secondary mechanical anchorage. Accordingly, PMMA usual only has the primary mechanical anchorage after application in fixation of artificial joints to the host bone. Active or over weight patient with implants fixed with PMMA are at risk from mantle failure, which occurs in 5% of all total joint replacement patients postoperatively by 10 years (Dorr et al., 1994). Bone cement of CPC approach exhibits a suitable degradation rate that allows the CPC to degrade properly and release Ca and P ions that will enhance bone formation in the early stage and get the secondary mechanical anchorage. Simultaneously, the CPC graft provides a greater bone contact surface, bridging the bone tissue to the Ti surface and thereby increasing the stabilization of Ti stem. This study clearly confirms the hypothesis that CPC graft

reinforces the prosthesis fixation process and facilitates osteointegration than the autograft. However, the routine use of CaP-based bone cements is not currently recommended for load-bearing condition directly. Because the CPC graft owns low resistance against flexural, tractive, and shear forces compared to PMMA, there is a higher risk of cement brittle failure and subsequent loss of restoration.

Conclusion

The calcium phosphate bone cement could promote structural stability and facilitate the biological bonding of growing bone tissue in a rabbit femur implantation model. We conclude that the better osteointegration of Ti implants at an early stage may be improved by reinforcement with the calcium-phosphate cement than the autograft alternatives.

References

[1] Albrektsson T BP, Hansson H, Kasemo B, Larsson K, Lundstrom I, McQueen D and Skalak R. The interface of inorganic implants in vivo; titanium implants in bone. . Annals of biomedical engineering 1983;11:27.
[2] Bragdon CR, Doherty AM, Rubash HE, Jasty M, Li XJ, Seeherman H, et al. The efficacy of BMP-2 to induce bone ingrowth in a total hip replacement model. Clin Orthop Relat Res 2003:50-61.
[3] Lappalainen R, Santavirta SS. Potential of coatings in total hip replacement. Clin Orthop Relat Res 2005:72-9.
[4] Urban RM, Jacobs JJ, Tomlinson MJ, Gavrilovic J, Black J, Peoc'h M. Dissemination of wear particles to the liver, spleen, and abdominal lymph nodes of patients with hip or knee replacement. J Bone Joint Surg Am 2000;82:457-76.
[5] Mak KH, Wong TK, Poddar NC. Wear debris from total hip arthroplasty presenting as an intrapelvic mass. J Arthroplasty 2001;16:674-6.
[6] Keel SB, Jaffe KA, Petur Nielsen G, Rosenberg AE. Orthopaedic implant-related sarcoma: a study of twelve cases. Mod Pathol 2001;14:969-77.
[7] Ritter MA, Albohm MJ, Keating EM, Faris PM, Meding JB. Comparative outcomes of total joint arthroplasty. J Arthroplasty 1995;10:737-41.
[8] Jaffin RA, Berman CL. The excessive loss of Branemark fixtures in type IV bone: a 5-year analysis. J Periodontol 1991;62:2-4.
[9] Mori H, Manabe M, Kurachi Y, Nagumo M. Osseointegration of dental implants in rabbit bone with low mineral density. J Oral Maxillofac Surg 1997;55:351-61; discussion 62.
[10] Kobayashi S, Saito N, Horiuchi H, Iorio R, Takaoka K. Poor bone quality or hip structure as risk factors affecting survival of total-hip arthroplasty. Lancet 2000;355:1499-504.
[11] Barlas KJ, Ajmi QS, Bagga TK, Howell FR, Roberts JA, Eltayeb M. Association of intra-operative metaphyseal fractures with prosthesis size during hemiarthroplasty of the hip. J Orthop Surg (Hong Kong) 2008;16:30-4.
[12] Pilliar RM, Lee JM, Maniatopoulos C. Observations on the effect of movement on bone ingrowth into porous-surfaced implants. Clin Orthop Relat Res 1986:108-13.
[13] Kendrick JB, 2nd, Noble PC, Tullos HS. Distal stem design and the torsional stability of cementless femoral stems. J Arthroplasty 1995;10:463-9.
[14] Jasty M, Bragdon C, Burke D, O'Connor D, Lowenstein J, Harris WH. In vivo skeletal responses to porous-surfaced implants subjected to small induced motions. J Bone Joint Surg Am 1997;79:707-14.
[15] Learmonth ID, Young C, Rorabeck C. The operation of the century: total hip replacement. Lancet 2007;370:1508-19.

[16] Lu JX, Huang ZW, Tropiano P, Clouet D'Orval B, Remusat M, Dejou J, et al. Human biological reactions at the interface between bone tissue and polymethylmethacrylate cement. J Mater Sci Mater Med 2002;13:803-9.
[17] Cherng AM, Chow LC, Takagi S. In vitro evaluation of a calcium phosphate cement root canal filler/sealer. J Endodont 2001;27:613-5.
[18] Friedman CD, Costantino PD, Jones K, Chow LC, Pelzer HJ, Sisson GA, Sr. Hydroxyapatite cement. II. Obliteration and reconstruction of the cat frontal sinus. Arch Otolaryngol Head Neck Surg 1991;117:385-9.
[19] Xu HH, Quinn JB, Takagi S, Chow LC. Synergistic reinforcement of in situ hardening calcium phosphate composite scaffold for bone tissue engineering. Biomaterials 2004;25:1029-37.
[20] Costantino PD, Friedman CD, Jones K, Chow LC, Pelzer HJ, Sisson GA, Sr. Hydroxyapatite cement. I. Basic chemistry and histologic properties. Arch Otolaryngol Head Neck Surg 1991;117:379-84.
[21] Hamanishi C, Kitamoto K, Ohura K, Tanaka S, Doi Y. Self-setting, bioactive, and biodegradable TTCP-DCPD apatite cement. Journal of Biomedical Materials Research 1996;32:383-9.
[22] Hong YC, Wang JT, Hong CY, Brown WE, Chow LC. The periapical tissue reactions to a calcium phosphate cement in the teeth of monkeys. J Biomed Mater Res 1991;25:485-98.
[23] Lu J, Descamps M, Dejou J, Koubi G, Hardouin P, Lemaitre J, et al. The biodegradation mechanism of calcium phosphate biomaterials in bone. J Biomed Mater Res 2002;63:408-12.
[24] Mermelstein LE, Chow LC, Friedman C, Crisco JJ, III. The reinforcement of cancellous bone screws with calcium phosphate cement. J Orthop Trauma 1996;10:15-20.
[25] Moore DC, Frankenburg EP, Goulet JA, Goldstein SA. Hip screw augmentation with an in situ-setting calcium phosphate cement: an in vitro biomechanical analysis. J Orthop Trauma 1997;11:577-83.
[26] Chen WC, Lin JH, Ju CP. Transmission electron microscopic study on setting mechanism of tetracalcium phosphate/dicalcium phosphate anhydrous-based calcium phosphate cement. J Biomed Mater Res A 2003;64:664-71.
[27] Lin DJ, Chuang CC, Chern Lin JH, Lee JW, Ju CP, Yin HS. Bone formation at the surface of low modulus Ti-7.5Mo implants in rabbit femur. Biomaterials 2007;28:2582-9.
[28] Lee JW, Lin DJ, Ju CP, Yin HS, Chuang CC, Lin JH. In-vitro and in-vivo evaluation of a new Ti-15Mo-1Bi alloy. J Biomed Mater Res B Appl Biomater 2009;91:643-50.

[29] Overgaard S, Lind M, Glerup H, Bunger C, Soballe K. Porous-coated versus grit-blasted surface texture of hydroxyapatite-coated implants during controlled micromotion: mechanical and histomorphometric results. J Arthroplasty 1998;13:449-58.
[30] Sugiyama H, Whiteside LA, Kaiser AD. Examination of rotational fixation of the femoral component in total hip arthroplasty. A mechanical study of micromovement and acoustic emission. Clin Orthop Relat Res 1989:122-8.
[31] Ooms EM, Verdonschot N, Wolke JG, Van de Wijdeven W, Willems MM, Schoenmaker MF, et al. Enhancement of initial stability of press-fit femoral stems using injectable calcium phosphate cement: an in vitro study in dog bones. Biomaterials 2004;25:3887-94.
[32] Taniwaki Y, Takemasa R, Tani T, Mizobuchi H, Yamamoto H. Enhancement of pedicle screw stability using calcium phosphate cement in osteoporotic vertebrae: in vivo biomechanical study. J Orthop Sci 2003;8:408-14.
[33] Hoshikawa A, Fukui N, Fukuda A, Sawamura T, Hattori M, Nakamura K, et al. Quantitative analysis of the resorption and osteoconduction process of a calcium phosphate cement and its mechanical effect for screw fixation. Biomaterials 2003;24:4967-75.
[34] Plenk H, Jr. Prosthesis-bone interface. J Biomed Mater Res 1998;43:350-5.
[35] Okumura M, Ohgushi H, Dohi Y, Katuda T, Tamai S, Koerten HK, et al. Osteoblastic phenotype expression on the surface of hydroxyapatite ceramics. J Biomed Mater Res 1997;37:122-9.

Figure legends

Figure 1 Illustration of the implantation site and histological section position.

Figure 2 A schematic diagram of the pull-out test apparatus involved the following steps: 1. screwing the pin and used a rig to ensuring alignment, 2. pouring in cold resin to fill the mold using a 0 ^{o}C water bath, 3. pulling out. The system was operated at continuously rinsing with phosphate buffer solution.

Figure 3 Pull-out strengths for the Ti stem at 1st, 4th, 12th, 26th and 70th postoperative week. Statistically different with increasing implantation time for both groups ($p<0.0001$). CPC groups comparison: 12w>4w, 26w>12w; Autografts: 12w>4w, 26w>12w, 70w>26w.

Figure 4 Radiographs and fresh sections (cranial view) of 1 week histological samples for the (a) autograft and (b) CPC group. (Scale bar = 10 mm).

Figure 5 H&E stains of paraffin sections at 1st, 4th, and 12th week. The first (a~c) and second row show section II for the respective autograft and CPC groups; and the last row (g~i) shows section III for PMMA implantation. fibrous stroma: F, New bone: NB, vascular tissue: V, CPC isolated islands: marked arrows.

Figure 6 Percentages of bone area (BA) and bone to implant contact length (BIC) of CPC and autograft groups at 1st, 4th, 12th, 26th, and 70th week post implantation (n=4). Statistically significant difference between both groups is marked by ◇ for BA and ↓ for BIC; ★ means $p > 0.05$ of BICs within the region.

Figure 7 Photographs of toludine blue stained section I of CPC groups. Residual cement was covered with bone tissues (a), cement was captured by macrophages (arrows) (b) at 1st week. After 12 weeks post-operation, the residual cement augment the peripheral bone tissue (c), the edge of the cement was indented by a new osteon formation (marked by asterisk) (d).

Figure 8 Immunohistochemically (IHC) stained sections of 4 weeks samples stained with anti-vimentin (a) and anti-vitamin D receptor (VDR) (b). Laser confocal images (Villanueva Bone Stain) after 4 weeks (c) and 12 weeks (d) implantation. Osteocytes: light yellow; Osteoid/collagens: pink; CPC/mineralized bone: green; Pores and crevices: blue. Ob: osteoblasts and marked by arrowhead; OC: osteoclast; Os: osteocytes; Pc: progenitor cell.

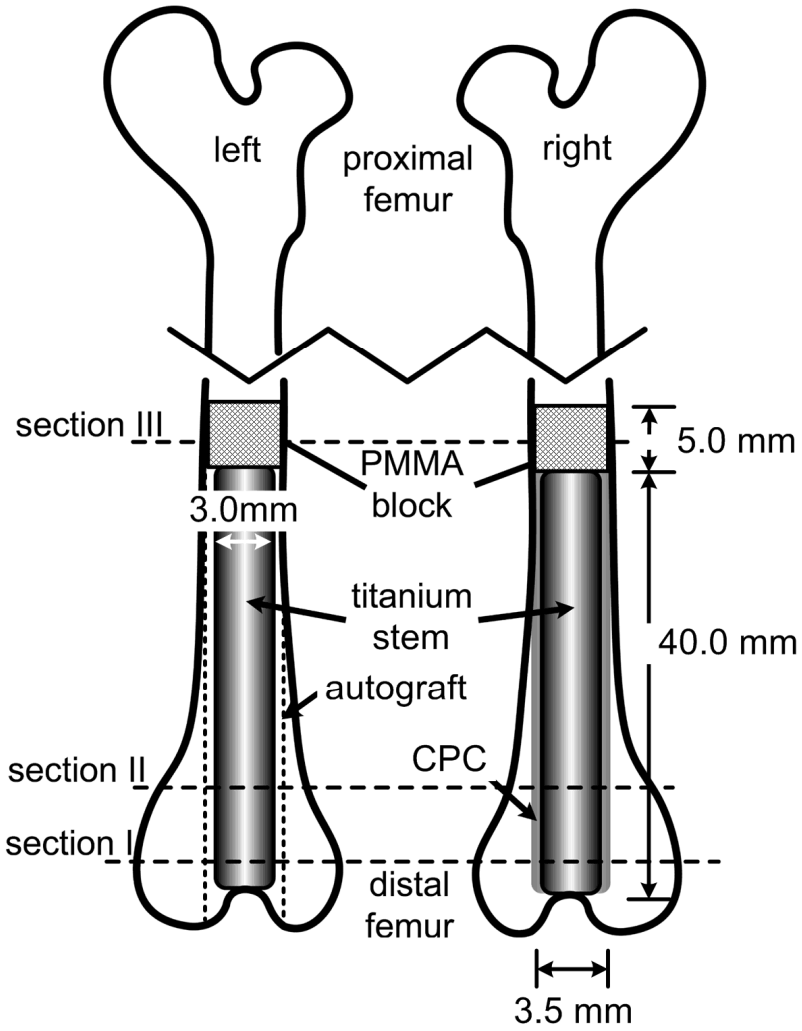

Figure 1 Illustration of the implantation site and histological section position.

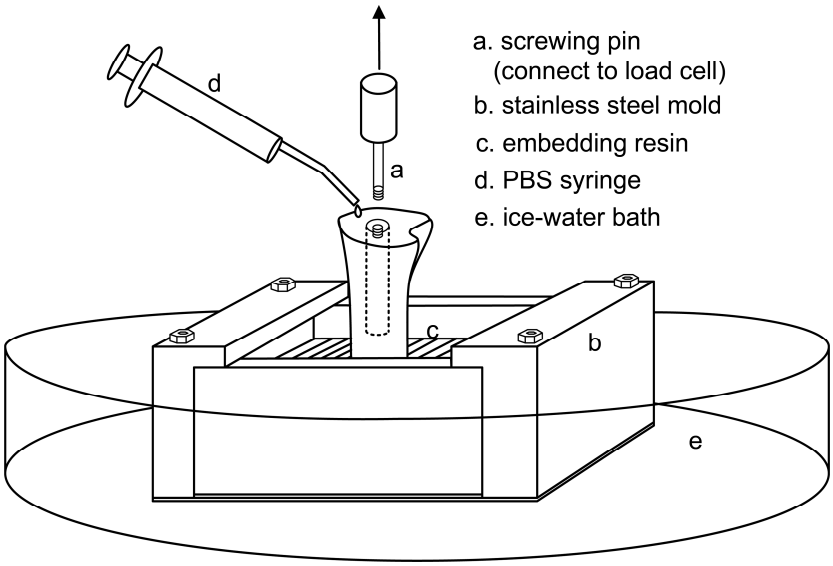

Figure 2 A schematic diagram of the pull-out test apparatus involved the following steps: 1. screwing the pin and used a rig to ensuring alignment, 2. pouring in cold resin to fill the mold using a 0 ^{o}C water bath, 3. pulling out. The system was operated at continuously rinsing with phosphate buffer solution.

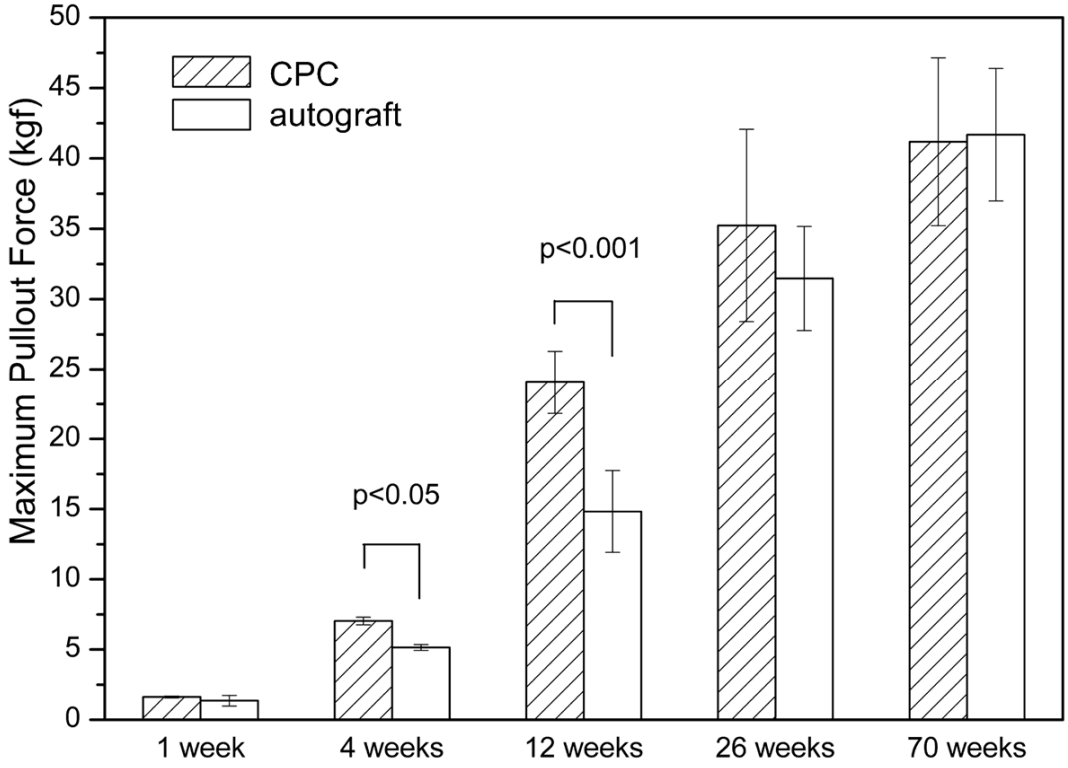

Figure 3 Pull-out strengths for the Ti stem at 1st, 4th, 12th, 26th and 70th postoperative week. Statistically different with increasing implantation time for both groups ($p<0.0001$). CPC groups comparison: 12w>4w, 26w>12w; Autografts: 12w>4w, 26w>12w, 70w>26w.

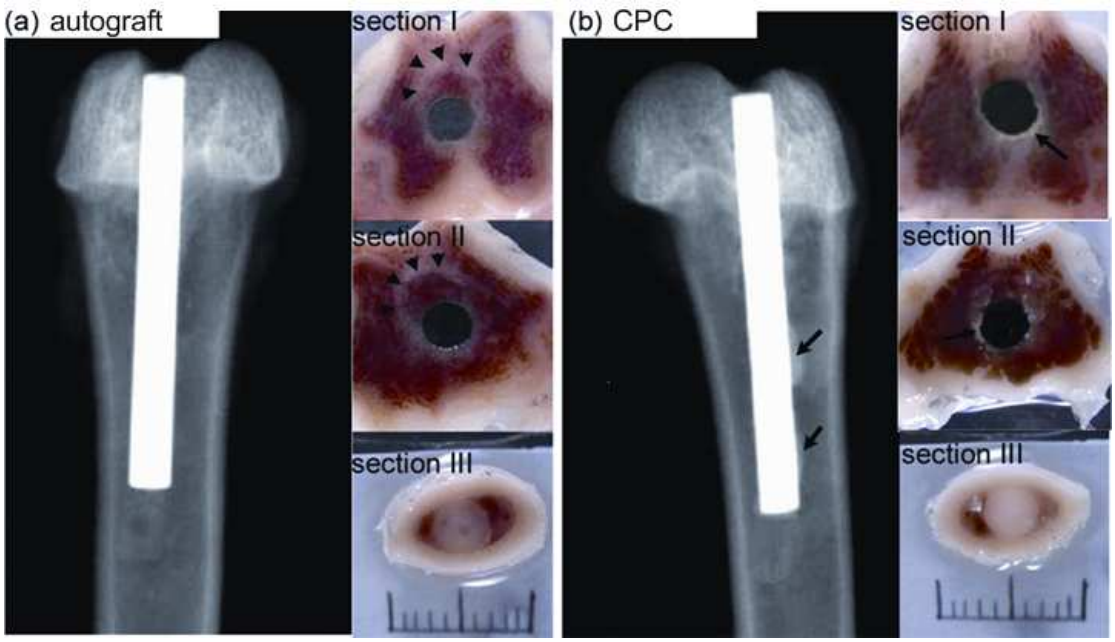

Figure 4 Radiographs and fresh sections (cranial view) of 1 week histological samples for the (a) autograft and (b) CPC group. (Scale bar = 10 mm).

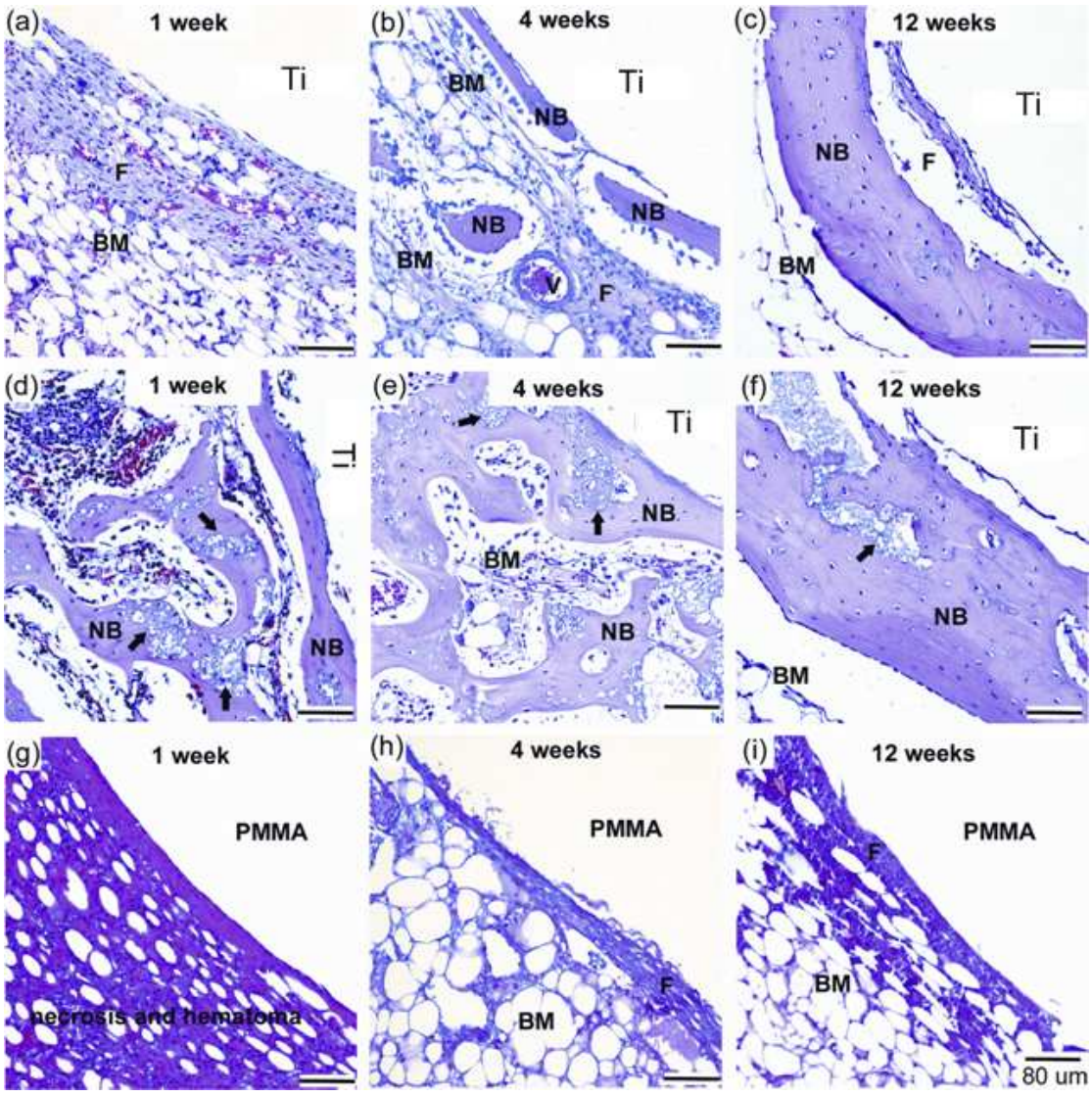

Figure 5 H&E stains of paraffin sections at 1st, 4th, and 12th week. The first (a~c) and second row show section II for the respective autograft and CPC groups; and the last row (g~i) shows section III for PMMA implantation. fibrous stroma: F, New bone: NB, vascular tissue: V, CPC isolated islands: marked arrows.

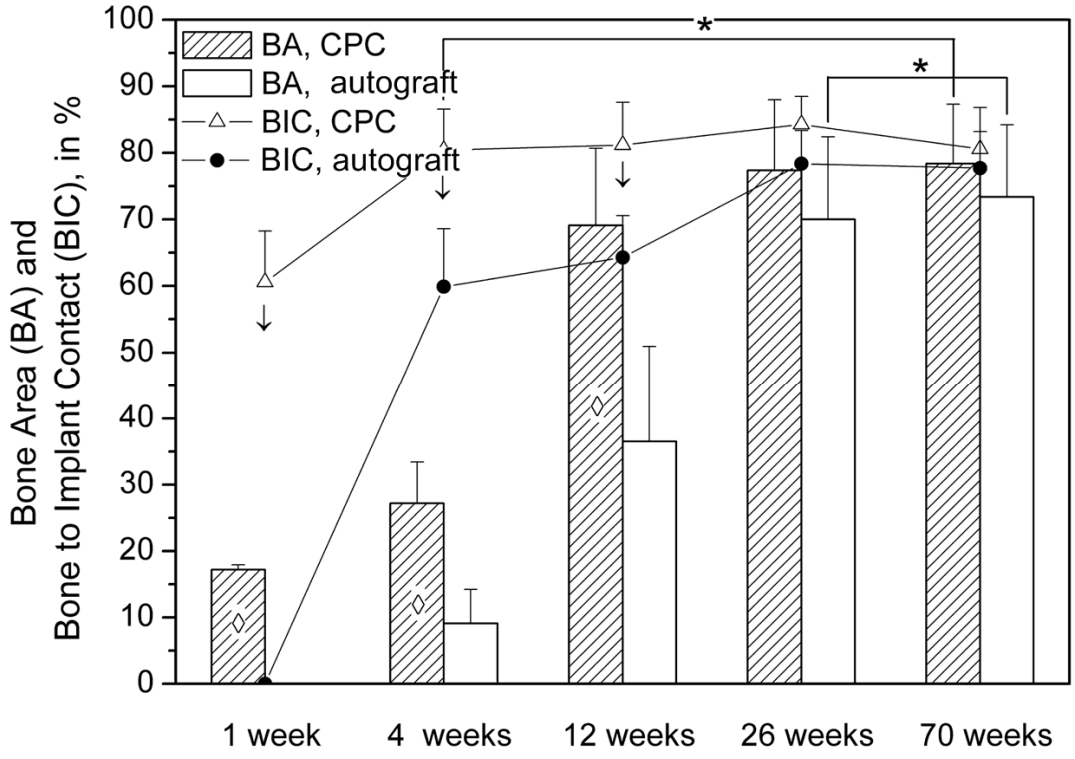

Figure 6 Percentages of bone area (BA) and bone to implant contact length (BIC) of CPC and autograft groups at 1st, 4th, 12th, 26th, and 70th week post implantation (n=4). Statistically significant difference between both groups is marked by ◇ for BA and ↓ for BIC; ★ means $p > 0.05$ of BICs within the region.

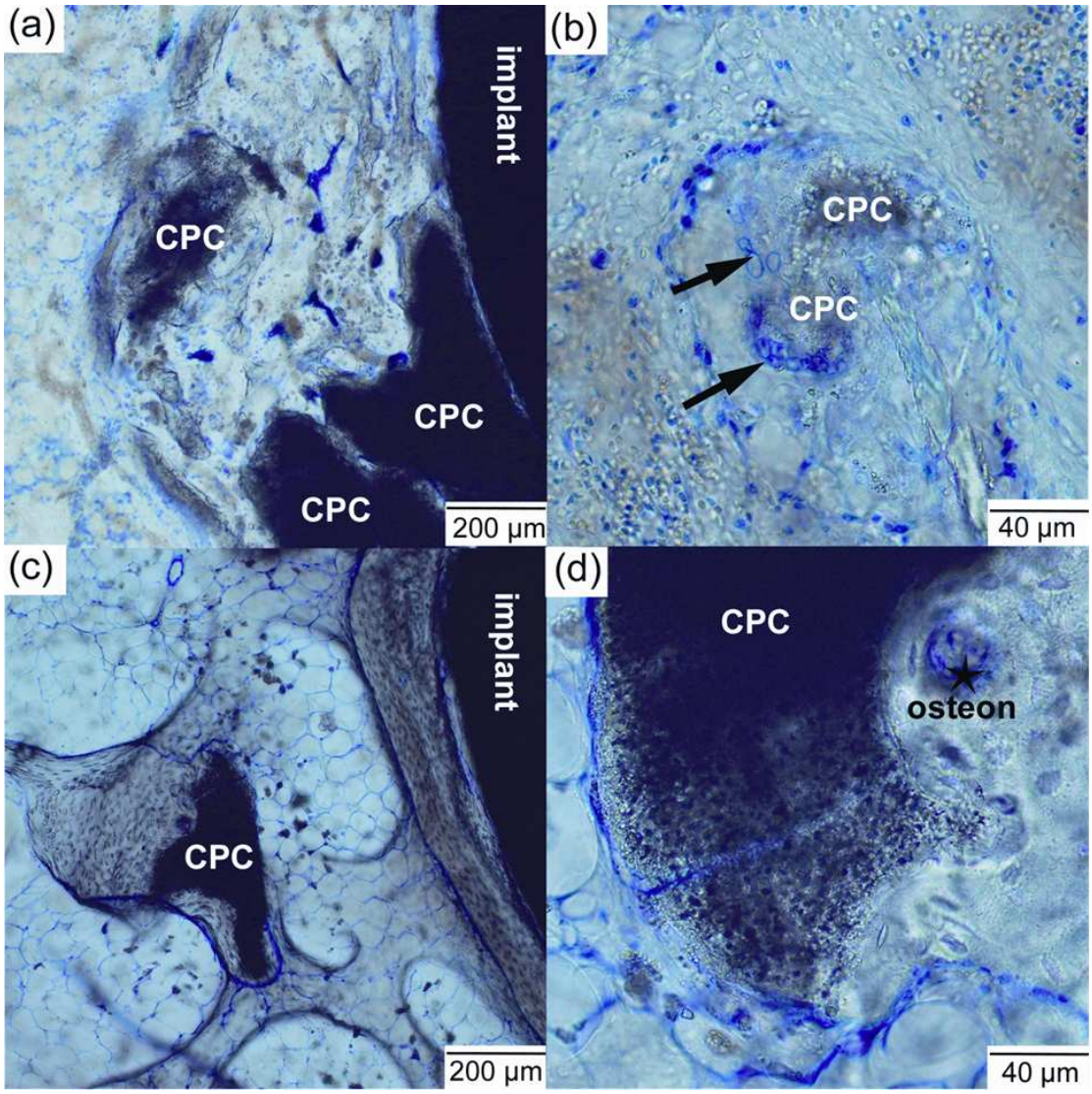

Figure 7 Photographs of toludine blue stained section I of CPC groups. Residual cement was covered with bone tissues (a), cement was captured by macrophages (arrows) (b) at 1st week. After 12 weeks post-operation, the residual cement augment the peripheral bone tissue (c), the edge of the cement was indented by a new osteon formation (marked by asterisk) (d).

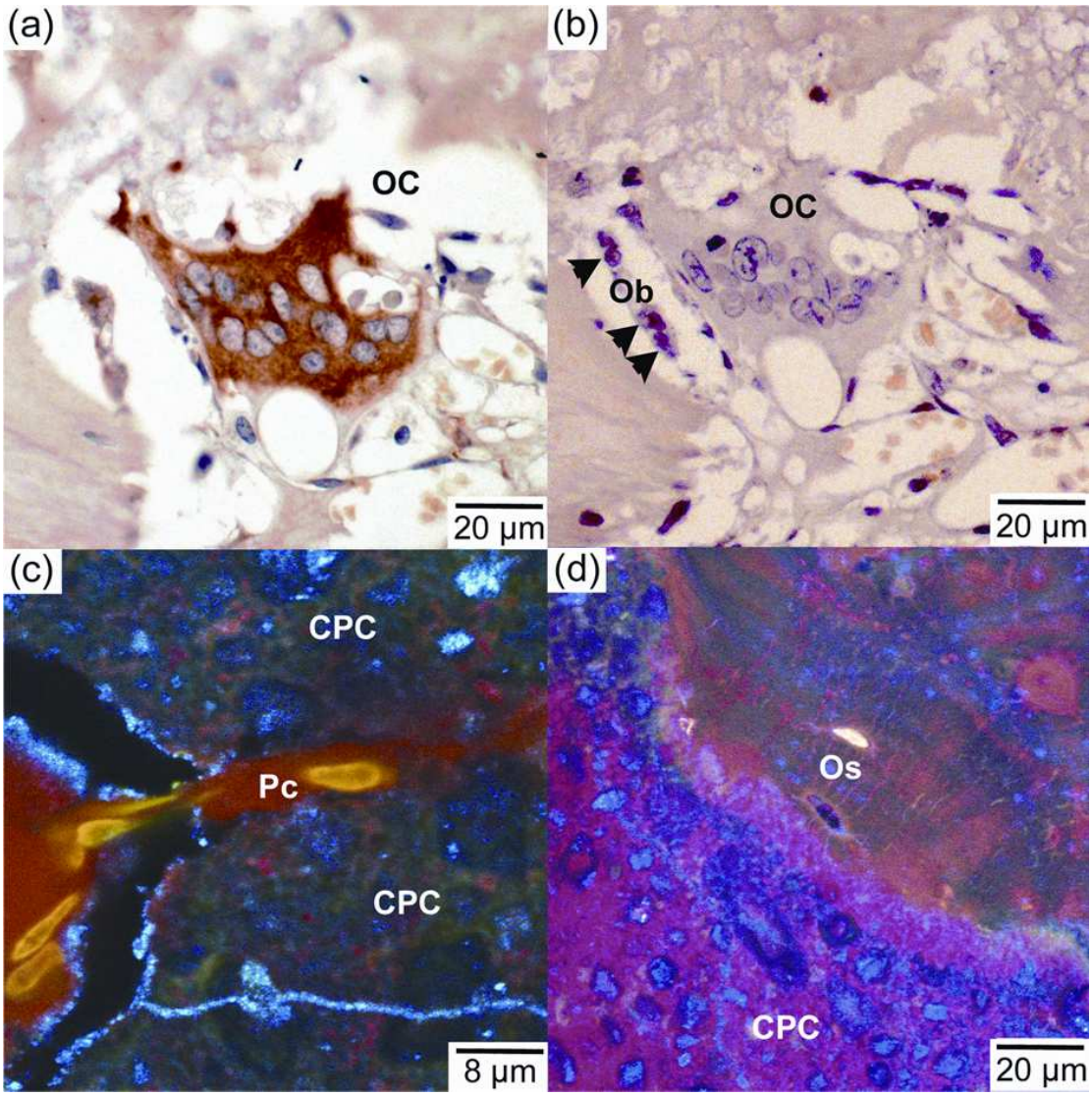

Figure 8 Immunohistochemically (IHC) stained sections of 4 weeks samples stained with anti-vimentin (a) and anti-vitamin D receptor (VDR) (b). Laser confocal images (Villanueva Bone Stain) after 4 weeks (c) and 12 weeks (d) implantation. Osteocytes: light yellow; Osteoid/collagens: pink; CPC/mineralized bone: green; Pores and crevices: blue. Ob: osteoblasts and marked by arrowhead; OC: osteoclast; Os: osteocytes; Pc: progenitor cell.